land

MDPI

Communication

Erosion Modelling Indicates a Decrease in Erosion Susceptibility of Historic Ridge and Furrow Fields near Albershausen, Southern Germany

Johannes Schmidt [1,2,*,†], Nik Usmar [1,†], Leon Westphal [1,†], Max Werner [1,†], Stephan Roller [3], Reinhard Rademacher [4], Peter Kühn [5], Lukas Werther [3] and Aline Kottmann [6]

1 Institute of Geography, Leipzig University, 04103 Leipzig, Germany
2 Historic Anthropospheres Working Group, Leipzig Lab, Leipzig University, 04107 Leipzig, Germany
3 Institute of Prehistory, Early History and Medieval Archaeology, Eberhard-Karls-Universität, 72070 Tübingen, Germany
4 County Archaeology, District Administration, 73008 Göppingen, Germany
5 Research Area Geography, Soil Science and Geomorphology, Eberhard-Karls-Universität, 72070 Tübingen, Germany
6 Archaeology, State Office for Cultural Heritage Baden-Wuerttemberg, 73728 Esslingen, Germany
* Correspondence: j.schmidt@uni-leipzig.de
† These authors contributed equally to this work.

Abstract: Ridge and furrow fields are land-use-related surface structures that are widespread in Europe and represent a geomorphological key signature of the Anthropocene. Previous research has identified various reasons for the intentional and unintentional formation of these structures, such as the use of a mouldboard plough, soil improvement and drainage. We used GIS-based quantitative erosion modelling according to the Universal Soil Loss Equation (USLE) to calculate the erosion susceptibility of a selected study area in Southern Germany. We compared the calculated erosion susceptibility for two scenarios: (1) the present topography with ridges and furrows and (2) the smoothed topography without ridges and furrows. The ridges and furrows for the studied site reduce the erosion susceptibility by more than 50% compared to the smoothed surface. Thus, for the first time, we were able to identify lower soil erosion susceptibility as one of the possible causes for the formation of ridge and furrow fields. Finally, our communication paper points to future perspectives of quantitative analyses of historical soil erosion.

Keywords: historic soil erosion; USLE; Anthropocene; Archaeology; Wölbäcker; ridge and furrow; historic land use; GIS; erosion management; historic anthroposphere

check for updates

Citation: Schmidt, J.; Usmar, N.; Westphal, L.; Werner, M.; Roller, S.; Rademacher, R.; Kühn, P.; Werther, L.; Kottmann, A. Erosion Modelling Indicates a Decrease in Erosion Susceptibility of Historic Ridge and Furrow Fields near Albershausen, Southern Germany. *Land* **2023**, *12*, 544. https://doi.org/10.3390/land12030544

Academic Editors: Bellotti Piero and Alessia Pica

Received: 25 January 2023
Revised: 15 February 2023
Accepted: 20 February 2023
Published: 23 February 2023

1. Introduction

Erosion caused by surface runoff leads to a serious loss of soil based ecosystem services. Areas of lower historical soil erosion are valuable areas of landscape and biodiversity resilience [1]. In the course of the current climate change, especially due to changing precipitation patterns and intensive land use, the average soil loss in Central Europe is expected to increase significantly [2,3]. The question of historical cultivation forms and their effects on soil erosion has so far been answered mainly qualitatively [4–7]. Models that simulate erosion quantitatively have existed for some time with the introduction of the USLE (Universal Soil Loss Equation) by Wischmeier and Smith [8] and the German adaption ABAG (*Allgemeine Bodenabtragsgleichung*) [9]. Beside actualistic studies [10–12], an application of such a concept to historical geomorphological conditions are rare [13,14].

As land use and topographic properties are crucial factors estimating soil erosion [15], the imprint of historical cultivation techniques in topographic properties are still important factors. In several areas of Germany [16–19], but also in other parts of Europe and beyond [6,18,20–22], large parts of former ridge and furrow field systems are still preserved. The most evident structures are ridge and furrow fields, which consist of several parallel ridge structures of considerable length (up to 700 m) and relatively small width (about 5–20 m), separated from each other by rather small furrows. They are clearly visible in LiDAR (Light Detection and Ranging) images [16,18] and characterise large parts of present-day meadow landscapes, also on low mountain slopes, where they have been well preserved through extensive use or afforestation after these fields were abandoned [23]. Due to their longevity and enormous spatial extent, they can be considered as a geomorphological key signature of the Anthropocene [24].

Origins and reasons for the establishment of ridge and furrow fields in low mountain ranges as well as path dependencies to the present appearance of the landscape are the focus of a collaborative research project in the district of Göppingen [25]. So far, various explanations for their establishment have been discussed in the literature: A common view sees a causal link between the mouldboard plough with fixed, non-turning ploughshare and long strip fields: it is argued that the fact that this type of plough led to an accumulation of clods of soil in the middle of the plots and the fact that the turning manoeuvres at the end of the field required a lot of energy, led to an elongated shape of the plots that required fewer trips for each owner [26,27]. Apart from the fact that ridge and furrow fields can also be formed by other types of soil tillage, additional causes are also discussed such as the function as boundary markers within open field systems [26], the improvement of water management or at least the increase of internal hydrological variability to secure crop yields [27] and the accumulation of organic fertiliser [21,28].

Therefore, we present a case study, where historic ridge and furrow fields are still visible in a loess landscape with high soil fertility. We focused on a field system with well-preserved ridge and furrow fields in the municipality of Albershausen, southern Germany (in total, c. 13 % of the area is still covered with remains of ridge and furrow structures). Many of the ridge and furrow fields there were oriented perpendicular to the slope, raising the question of whether this orientation was deliberately chosen to reduce erosion of the vital soil and humus cover and/or to support the run-off of excess rainwater. To answer this question, we used a GIS-based USLE approach to model and compare the erosion susceptibility using a digital elevation model of the present topography and a smoothed topography without ridge and furrow structures.

2. Materials and Methods

2.1. Study Area

The plot *Höfelbett* is located northwest to the village of Albershausen on the fringe of the Swabian Karst. It has been mentioned in 1476/77 for the first time in a stock book [29] and is nowadays used as an extensive orchard, which helped the old field system to survive in a well preserved and visible way up to today (Figure 1). Albershausen was first mentioned in 1275 in the *liber decimationis* [29] but may be of older, presumably early medieval origin due to its characteristic place name suffix-*hausen* [30]. One of the questions asked was how long has the field system been in use for. Today the region is characterised by a Cfb climate with 1058 mm mean annual precipitation and a mean annual temperature of 9.3 °C. The wettest months are in spring and summer. Heavy rainfall is also most frequent during this period [31,32]. The geology of the *Höfelbett* consists of a pisolith-rich claystone (Obtusus Clay Formation) on the upper slope and sandstone (Angulate Sandstone Formation, Lower Jurassic) on the middle to lower slope [33]. Both formations are covered by a lower periglacial layer (mainly clay loam with intercalated sandstone fragments) and an upper periglacial layer consisting mainly of loess loam with a few small sandstone fragments and pisoliths. Eroded Luvisols frequently occur in areas with thicker loess loam, while stagnic Luvisols and Vertisols are developed in more clayey and Cambisols in more sandy substrates. The boundaries of the individual fields and today's parcels are identical to the field boundaries from the original cadastre of 1828 [34]. Their size varies considerably with lengths between 86 and nearly 400 m and widths between 8 and 20 m.

The individual ridges are still between 25 and 80 cm high (Figure 1). The plot *Höfelbett* is situated at a North-East facing slope with a mean slope angle of c. 5° and cut off on the north by a narrow valley leading east. Between 2020 and 2022 five archaeological trenches were opened as accompanying measures of the development of the site. The soils were described according to WRB [35] and samples were taken for dating, soil chemical and soil physical analyses as well as for archaeobotanical and ancient DNA analyses [25].

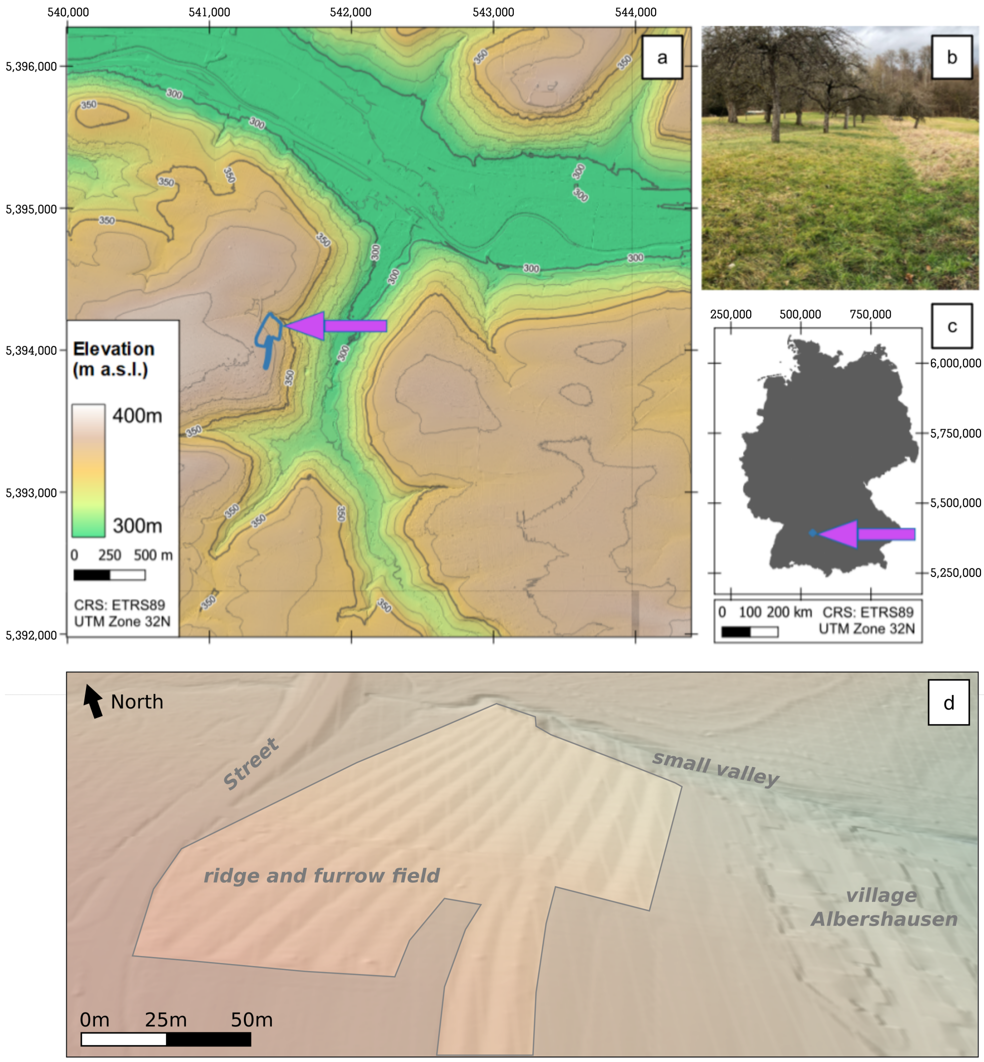

Figure 1. (**a**) Topographical map of the area surrounding the plot "Höfelbett" in Albershausen based on LiDAR DEM data (©www.lgl-bw.de (accessed on 24 January 2023)) [36]. The blue line frames the plot *Höfelbett*. (**b**) Picture of the plot with visible ridge- and furrow structures. (**c**) Location of the study area within Germany. (**d**) 3D view of the study area (elevation and hillshade) based on LiDAR DEM data (©www.lgl-bw.de (accessed on 24 January 2023)).

2.2. Data

To model soil erosion, the USLE requires four factors to be multiplied for any given point in the study area (Table 1): slope gradient and length (LS-factor), soil erodibility (K-factor), rainfall erosivity (R-factor) and land cover (C-factor) [8]. To calculate the LS-factor, we used a LiDAR DEM provided by LGL (*Landesamt für Geoinformation und Landesentwicklung Baden-Württemberg*) [36]. This DEM has a spatial resolution of 0.5 m and is therefore suitable to accurately depict the ridge and furrow structures in the study area [16,18]. For the second factor of the USLE, R-factor, we used a data set from the German Weather Service (DWD - *Deutscher Wetterdienst*), which was derived from radar measurements of precipitation. This dataset has a spatial resolution of 1000 m due to the low variability of rainfall erosivity on a local scale [37,38]. The complete study area lies within a single cell of this data set, which appoints a value of $R = 104.497864915$ kJ/m^2/mm. The K-factor data set has been created by the German Federal Institute for Geosciences and Natural Resources (BGR - *Bundesanstalt für Geowissenschaften und Rohstoffe*) based on their land use stratified soil map of Germany at scale 1:1,000,000 and according to *DIN 19708:2005-02* [39]. This data set has a spatial resolution of 250 m and offers one value for the complete study area which is $K = 0.22912$ (t/ha)/(N/ha). Concerning C-Factor, there are various possible approaches to calculate modern day values depending on the data available [40–43]. As stated earlier, we assume that historical land use was different from the meadow orchard found there today. In absence of historical data accurately describing early medieval farming practices and arable crops in the area, we assigned $C = 0.2$. This value is meant to represent wheat farming with standard tillage practices as implemented in the Europe-wide RUSLE 2015 soil erosion study [42].

Table 1. Basic USLE factor data product acquisition and description.

Data Product	Data Source	Availability	Spatial Resolution (m)
LiDAR DEM	LGL [36]	upon request	0.5
R-factor	DWD [37]	open access	1000
K-factor	BGR [39]	open access	250
C-factor	ESDAC [42]	open access	-

2.3. Modelling Routine

To approximate the influence of ridge and furrow structures on soil erosion for our study area, we chose to simulate soil erosion rates under two scenarios (procedure in Figure 2): (1) The first is the *present surface* scenario, which represents the relief of the study area exactly as it is now, including the ridge and furrow structures. (2) The second scenario is called *smoothed surface*, which describes soil erosion rates for the study area using a virtually smoothed surface that does not include the ridge and furrow structures, while at the same time preserving the larger scale topographical properties of the study area. Therefore, we assume this smoothed surface to serve as an approximate model for the pre-ridge and furrow palaeosurface. The first step after acquiring all necessary data from the sources listed in Table 1 was to create the virtually smoothed surface in Quantum-GIS (QGIS). To do this, we applied the *Gaussian Filter* function [44] to the DEM using the following settings: *Standard Deviation = 50; Kernel Type = Circle; Radius = 20*. The *Gaussian Filter* and specific settings were chosen by a trial and error approach. Methods mentioned in other publications [45,46] for slightly different objectives, e.g., the *Low pass Filter* changed the underlying relief more than necessary in order to smooth out only the ridge and furrow structures.

After the virtually smoothed surface had been created using the Gaussian Filter, we proceeded to use the USLE, for estimating soil erosion rates. In addition to the factors (K, R and C), described above, the slope gradient and length (LS) is necessary for the calculation of the USLE [8]. K, R and C were gained from external data sets as shown in Table 1 and are used in both scenarios without alteration. As the K, R and C factors are independent from the shape of the surface and equal in both scenarios, LS must be the crucial factor in this study. For its calculation, we applied the exact same procedure to the present surface and the virtually smoothed surface. We used the function *LS-factor, field based* with the method of calculation set to *Wischmeier and Smith 1978* [8]. Hrabalikova et al. 2017 [47] found with empirical measurements that USLE models using this method for LS calculation predicted erosion most accurately in a manual and GIS environment. The settings were as follows: *Type of Slope = [0] local slope; Specific Catchment Area = [1] contour length dependent on aspect; Rill/Interrill Erosivity = 1; Stability = [0] stable.*

We then multiplied each of the two resulting LS-factor Layers with all other factors using *Raster Calculator* in QGIS (Figure 2). The extent was set to match the DEM-based catchment area of the plot *Höfelbett*. This provided two erosion models representing the *present surface* and *smoothed surface* scenarios.

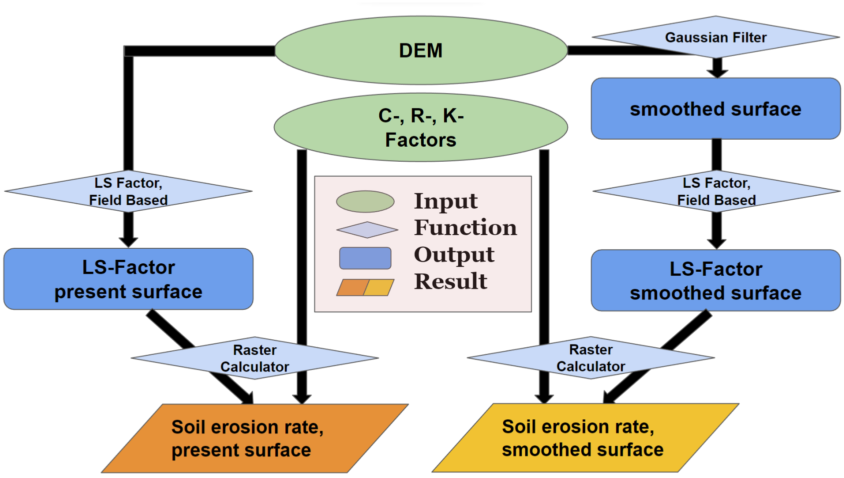

Figure 2. Flowchart of the GIS-based modelling procedure for both scenarios for calculating the potential soil erosion.

3. Results

The difference between our erosion model scenarios is the topography. In the calculation of the USLE, only the calculated LS factor differs. The smoothed surface model no longer shows ridges and furrows (Figure 3). However, the general topography of the slope is maintained. The drainage direction is therefore also preserved. In addition to the linear structures on the agricultural land, further anthropogenic structures such as buildings (visible on the western margin of Figure 3) have also been cleared away.

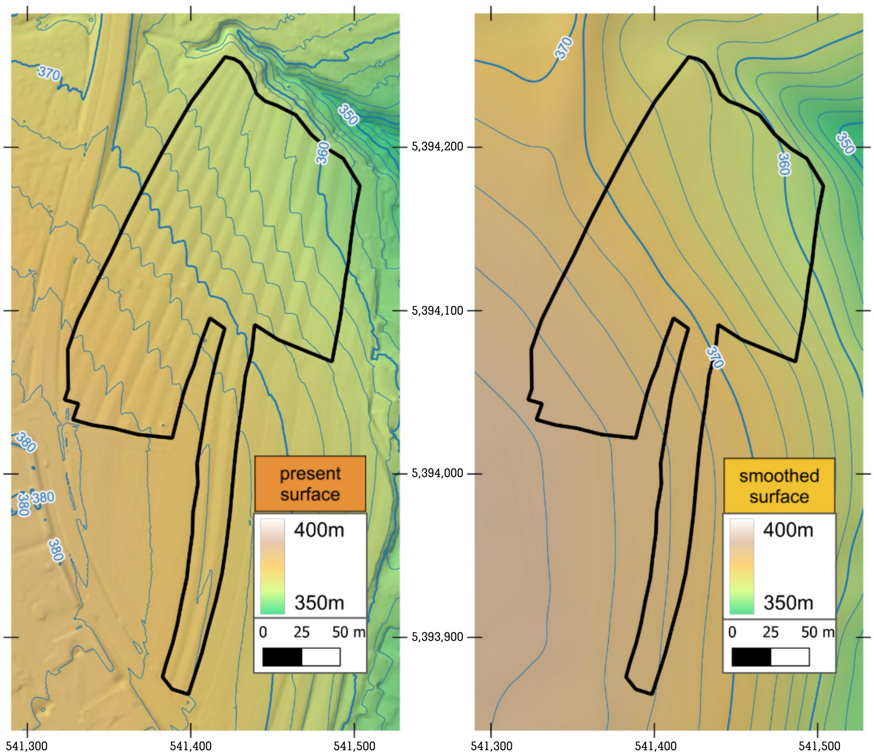

Figure 3. Comparison of the present (**left**) and smoothed (**right**) surface topography based on the LiDAR DEM (©www.lgl-bw.de (accessed on 24 January 2023)) [36]. The black line frames the classified cultural site within the plot *Höfelbett*.

The *present surface* scenario model (Figure 4 left) shows the highest erosion rates on top of the ridges of the ridge and furrow structures, with very low erosion rates in the furrows. Sharper edges of the ridges create extreme values in potential soil loss. In contrast, under the *smoothed surface* scenario, the rates are evenly low at the western, higher upper slope of the plot and gradually increase towards the east. The slope gradient is essentially constant across the plot (see Figure 3), so these differences must be a result of the increased slope length and connectivity. Maximum values, comparable with extreme values from the *smoothed surface* scenario only appear in the northernmost part in context of the steeps slopes of the small valley at the northern margin (Figure 4).

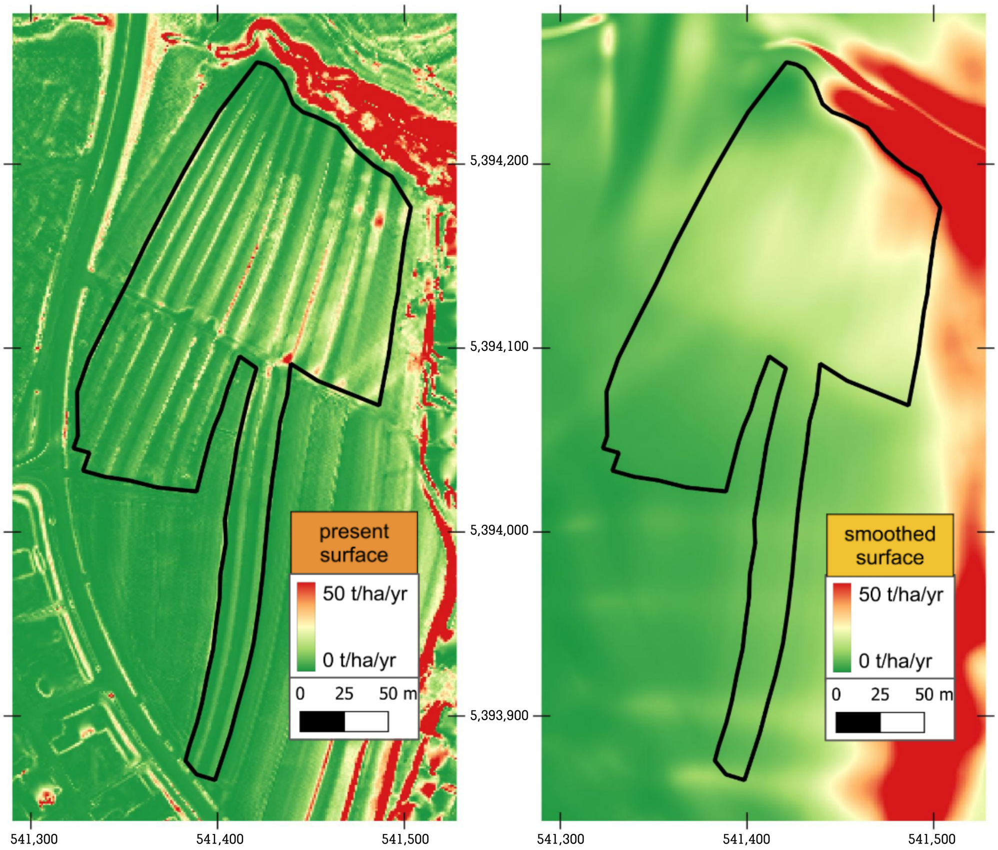

Figure 4. Maps of the two (**left**: present surface, **right**: smoothed surface) erosion models for the study area. The red-to-green colour range shows the mean annual soil loss. The black line frames the cultural site within the plot *Höfelbett*.

4. Discussion

4.1. Erosion Susceptibility of Ridge and Furrow Structures

The reconstruction of a palaeosurface, based only on a deductive filtering approach, such as the Gaussian filter, can produce unintentional effects. The surface smoothing in the area of the bridge (at the northern margin of the map, Figure 3) shows insufficient removal. However, since the area of the bridge lies in the periphery of the catchment area of the *Höfelbett*, no bias of the results of the erosion model is to be expected. A coupled approach in building up a (ridge-and-furrow-free) palaeosurface should consider large linear structures and remove them accordingly [45,48,49].

Summary statistics for all raster cells (0.5 m spatial resolution as given by the LiDAR data) of the modelled potential soil loss show clear differences between both scenarios (Figure 5). The results suggest that the ridge and furrow structures reduce erosion by approximately 50% according to the arithmetic mean. However, the median is more meaningful because extreme values at the edges of the ridges are small scale and and may have been artificial outliers. The median shows a 3-fold increase for potential erosion for the smoothed surface scenario and a 3-fold decrease for the present surface with ridge and furrow features.

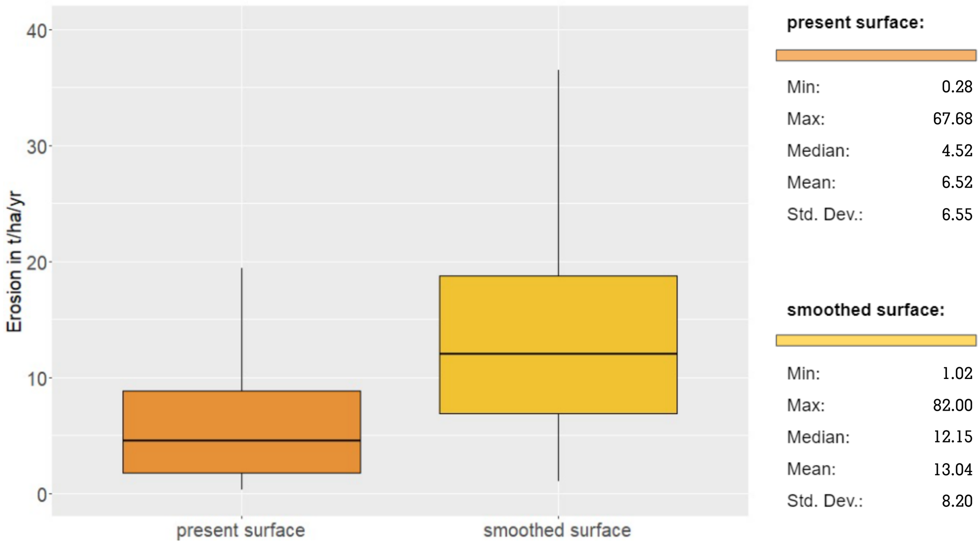

Figure 5. Boxplot and summary statistics of raster cell values of both erosion model scenarios.

It is clear that a topography structured by ridges and furrows significantly reduces erosion. Even today, the altered erosion rates through old ridges and furrows are noticeable [50,51]. Ridges and furrows have also been linked to changed erosion patterns [52], e.g., they were attributed to a potentially increased erosion through high landscape connectivity in times of increased cultivation during the 9th and 10th century AD on landscape scale [6]. In general, changing erosion rates can be quantified based on scenarios of historical land uses and their effects [14].

Compared to RUSLE calculations by ESDAC [53], both our *smoothed surface* and our *present surface* scenario models predict soil erosion rates above the European average for arable land of 2.46 t/ha/yr (see Figure 5). This difference of maximum values cannot be attributed to a single factor of our model. Generally, it seems that the combination of the USLE factors in our study leads to such high erosion rates compared to the European scale RUSLE calculations, which are more sensitive for surface runoff distribution [37,54,55].

Today, we still observe large areas with ridge and furrow fields in the district. There has been a conversion of arable land, including many ridge and furrow fields to grassland, orchards and also forests, which are of different origins and periods [56]. The late medieval desertification phase [57,58], but also the intensification and increased productivity of agriculture in the last century has significantly changed the structure of the rural areas and the extent of cultivated land. This conversion often occurred on slopes that were labour-intensive for arable farming [59] and resulted in large areas of ridge and furrow fields still being preserved in the study area.

4.2. Future Perspectives

1. We see a high potential to quantify landscape-altering processes such as erosion (as well as their geo-ecological consequences and yield changes) in a historical context using erosion models with different topographic scenarios. This will allow for a quantification of anthropogenic impacts, e.g., on hydrology and soil preservation, on a local scale and therefore contribute to global models of pathways to the Anthropocene.
2. In order to refine the validity of erosion models, it is crucial to adjust the USLE factors to the historical context. Information of the historical land use (C-factor) and land use techniques (P-factor) could be derived from local palaeoecological archives (e.g., pollen, phytoliths, sedimentary DNA, geo-biomarkers) as well as from archaeological and written sources [60,61]. The K-factor can be adjusted by

local, empirical sedimentological analyses of soil properties, especially because of the exposure of different soil horizons (with varying erodibility) during erosion phases. The reconstruction of a historical R-factor can be achieved using model scenarios of rainfall erosivity [62] but also accompanied by regional proxy-based palaeoclimatic reconstructions [63,64] and (semi-) quantitative data from written sources [65].

3. As our approach is based on the comparison of the present surface with a ridge and furrow-free smoothed surface, precise palaeosurface reconstructions are essential to improve the results. We encourage the use and adaptation of existing deductive, inductive and coupled surface modelling (see review in [45]) approaches to create supervised (cross-checked with historical and land use information) and reproducible *pre-modern* Digital Terrain Models with high spatial resolution.
4. One further hypothesis about the functions of ridge and furrow fields may be addressed using a similar approach: the assumption of a positive effect on the hydro management of soils. The furrows are meant to drain surface runoff from precipitation and the humus-rich ridges increased water storage capacities. Case modelling can generate quantitative data about such anthropogenic impacts on the soil moisture and proof historic *geo-engineering* on a local level.
5. The coupling of empirical sedimentological-geoarchaeological data of soil erosion and erosion models offers the chance of (i) a model verification and (ii) the examination to what extent parameters of the erosion model have to be adjusted. Therefore, we see field-based geomorphological, sedimentological and archaeological mappings and information gain indispensable. The link to soil geochemical laboratory results (e.g., soil organic matter) also allows the distribution of carbon stocks to be modelled using e.g., machine learning approaches in digital soil mapping [66,67].
6. To clarify the question of the extent to which erosion reduction contributes to the installation of ridges and furrows, a systematic mapping of ridge and furrow fields at (supra-) regional level is important. The comparison with geomorphological indices, such as slope, aspect, angle of the ridges and furrow to the slope, as well as geological-sedimentological characteristics allows the identification of common patterns.

5. Conclusions

For the first time, we have shown how valuable a quantitative erosion modelling approach can be for assessing what effects historic ridge and furrow fields can have on soil erosion. With a GIS-based erosion modelling approach based on the Universal Soil Loss Equation (USLE), we compared two scenarios with surface topographies in a small study area in Southern Germany: (1) The present topography with ridges and furrows and (2) the smoothed topography without ridges and furrows. This allowed us to show that historical land uses with ridges and furrows led to a strongly reduced erosion susceptibility. From this, we drew six key perspectives for future research on the topic of historical anthropospheres regarding ridge and furrow fields.

Author Contributions: Conceptualization: J.S., N.U., L.W. (Leon Westphal), M.W. and L.W. (Lukas Werther); methodology: J.S., N.U., L.W. (Leon Westphal) and M.W.; software: J.S., N.U., L.W. (Leon Westphal) and M.W.; validation: J.S., N.U., L.W. (Leon Westphal), M.W., P.K., A.K. and L.W. (Lukas Werther); formal analysis: J.S., N.U., L.W. (Leon Westphal) and M.W.; investigation: J.S., N.U., L.W. (Leon Westphal) and M.W.; resources: J.S., N.U., L.W. (Leon Westphal), M.W. and S.R.; data curation: J.S., N.U., L.W. (Leon Westphal), S.R. and M.W.; writing—original draft preparation: J.S., N.U., A.K, S.R. and P.K.; writing—review and editing: J.S., N.U., L.W. (Leon Westphal), M.W., A.K., L.W. (Lukas Werther) and P.K.; visualization: N.U., L.W. (Leon Westphal) and M.W.; supervision: J.S., A.K., L.W. (Lukas Werther), P.K. and R.R.; project administration: A.K., P.K., L.W. (Lukas Werther) and R.R.; funding acquisition: A.K. and R.R. All authors have read and agreed to the published version of the manuscript.

Funding: This research received no external funding. The Article Processing Charge (APC) was funded by Leipzig University within the program of Open Access publishing.

Data Availability Statement: The data presented in this study are available on request from the corresponding author. The data are not publicly available due to legal reasons.

Acknowledgments: We would like to thank Michael Weidenbacher (County Archaeology, District Administration, Göppingen) and Ralf Hesse (State Office for Cultural Heritage Baden-Wuerttemberg, Esslingen) for their support in the field and concerning data compilation. Furthermore, we thank Alexander Bolland for English spell checking. We thank four anonymous reviewers for their helpful comments.

Conflicts of Interest: The authors declare no conflict of interest.

References

1. Baude, M.; Meyer, B.C.; Schindewolf, M. Land use change in an agricultural landscape causing degradation of soil based ecosystem services. *Sci. Total Environ.* **2019**, *659*, 1526–1536. [CrossRef]
2. Uber, M.; Rössler, O.; Astor, B.; Hoffmann, T.; van Oost, K.; Hillebrand, G. Climate Change Impacts on Soil Erosion and Sediment Delivery to German Federal Waterways: A Case Study of the Elbe Basin. *Atmosphere* **2022**, *13*, 1752. [CrossRef]
3. Marcinkowski, P.; Szporak-Wasilewska, S.; Kardel, I. Assessment of soil erosion under long-term projections of climate change in Poland. *J. Hydrol.* **2022**, *607*, 127468. [CrossRef]
4. Larsen, A.; Robin, V.; Heckmann, T.; Fülling, A.; Larsen, J.R.; Bork, H.R. The influence of historic land-use changes on hillslope erosion and sediment redistribution. *Holocene* **2016**, *26*, 1248–1261. [CrossRef]
5. Dreibrodt, S.; Lubos, C.; Terhorst, B.; Damm, B.; Bork, H.R. Historical soil erosion by water in Germany: Scales and archives, chronology, research perspectives. *Quat. Int.* **2010**, *222*, 80–95. [CrossRef]
6. Brown, A.G. Colluvial and alluvial response to land use change in Midland England: An integrated geoarchaeological approach. *Geomorphology* **2009**, *108*, 92–106. [CrossRef]
7. Dotterweich, M. The history of soil erosion and fluvial deposits in small catchments of central Europe: Deciphering the long-term interaction between humans and the environment—A review. *Geomorphology* **2008**, *101*, 192–208. [CrossRef]
8. Wischmeier, W.H.; Smith, D.D. *Predicting Rainfall Erosion Losses—A Guide to Conservation Planning*; Agriculture Handbook; U.S. Department of Agriculture: Washington, DC, USA, 1978; Volume 537.
9. Schwertmann, U.; Vogl, W.; Kainz, M. *Bodenerosion durch Wasser: Vorhersage des Abtrags und Bewertung von Gegenmaßnahmen*; Eugen-Ulmer Verlag: Stuttgart, Germany, 1987.
10. Tetzlaff, B.; Friedrich, K.; Vorderbrügge, T.; Vereecken, H.; Wendland, F. Distributed modelling of mean annual soil erosion and sediment delivery rates to surface waters. *CATENA* **2013**, *102*, 13–20. [CrossRef]
11. Schmidt, S.; Alewell, C.; Meusburger, K. Monthly RUSLE soil erosion risk of Swiss grasslands. *J. Maps* **2019**, *15*, 247–256. [CrossRef]
12. Gericke, A.; Kiesel, J.; Deumlich, D.; Venohr, M. Recent and Future Changes in Rainfall Erosivity and Implications for the Soil Erosion Risk in Brandenburg, NE Germany. *Water* **2019**, *11*, 904. [CrossRef]
13. Favis-Mortlock, D.; Boardman, J.; Bell, M. Modelling long-term anthropogenic erosion of a loess cover: South Downs, UK. *Holocene* **1997**, *7*, 79–89. [CrossRef]
14. Ayala, G.; French, C. Erosion modeling of past land-use practices in the Fiume di Sotto di Troina river valley, north-central Sicily. *Geoarchaeology* **2005**, *20*, 149–167. [CrossRef]
15. Sun, W.; Shao, Q.; Liu, J.; Zhai, J. Assessing the effects of land use and topography on soil erosion on the Loess Plateau in China. *CATENA* **2014**, *121*, 151–163. [CrossRef]
16. Sittler, B. Revealing historical landscapes by using Airborne Laser Scanning: A 3D-Model of ridge and furrow in forests near Rastatt (Germany). *Int. Arch. Photogramm. Remote Sens. Spat. Inf. Sci.* **2004**, *8*, 258–261.
17. Schmoock, I.; Gehrt, E. Verbreitung und Charakterisierung der Wölbackerböden in Niedersachsen. Jahrestagung der DGB, Kom V. 2017. Available online: https://eprints.dbges.de/1271/ (accessed on 5 January 2023).
18. van Gils, H.; Kasielke, T. Historical parcellation and ridge-and-furrow relics of open strip-fields in the north-west European lowlands. *Landsc. Hist.* **2022**, *43*, 77–102. [CrossRef]
19. Langewitz, T.; Fülling, A.; Klamm, M.; Wiedner, K. Historical classification of ridge and furrow cultivation at selected locations in Northern and central Germany using a multi-dating approach and historical sources. *J. Archaeol. Sci.* **2020**, *123*, 105248. [CrossRef]
20. Catsadorakis, G.; Mougiakou, E.; Kizos, T. Ridge-and-Furrow Agriculture around Lake Mikri Prespa, Greece, in a European perspective. *J. Eur. Landsc.* **2021**, *2*, 7–20. [CrossRef]
21. Langewitz, T.; Wiedner, K.; Polifka, S.; Eckmeier, E. Pedological properties related to formation and functions of ancient ridge and furrow cultivation in Central and Northern Germany. *CATENA* **2021**, *198*, 105049. [CrossRef]
22. Palmer, R. A further case for the preservation of earthwork ridge-and-furrow. *Antiquity* **1996**, *70*, 436–440. [CrossRef]
23. Schreg, R. Mittelalterliche Feldstrukturen in deutschen Mittelgebirgslandschaften—Forschungsfragen, Methoden und Herausforderungen für Archäologie und Geographie. In *Agrarian Technology in the Medieval Landscape*; Klápště, J., Ed.; Brepols Publishers n.v: Turnhout, Belgium, 2016; pp. 351–370.

24. Brown, A.G.; Tooth, S.; Bullard, J.E.; Thomas, D.S.G.; Chiverrell, R.C.; Plater, A.J.; Murton, J.; Thorndycraft, V.R.; Tarolli, P.; Rose, J.; et al. The geomorphology of the Anthropocene: Emergence, status and implications. *Earth Surf. Process. Landf.* **2017**, *42*, 71–90. [CrossRef]
25. Kottmann, A.; Harding, S.; Kühn, P.; Marinova-Wolff, E.; Miller, C.E.; Nelle, O.; Rademacher, R.; Schreg, R.; Vogt, R.; Werther, L. *Untersuchungen der Wölbäcker im Gewann "Höfelbett" in Albershausen*; Archäologische Ausgrabungen in Baden-Württemberg: Darmstadt, Germany , 2020; pp. 322–326.
26. Ewald, K.C. Agrarmorphologische Untersuchungen im Sundgau (Oberelsass) unter besonderer Berücksichtigung der Wölbäcker. *Tätigkeitsbericht Der Nat. Ges. Baselland* **1968**, *2*, 9–178.
27. Bartussek, I. Die Gewölbten Ackerbeete in der historischen Landwirtschaft—Ihr Relikte und Nachwirkungen in der Gegenwart: Diploma Thesis. Ph.D. Thesis, Georg-August-Universität Göttingen, Göttingen, Germany, 1982.
28. Langewitz, T.; Wiedner, K.; Fritzsch, D.; Eckmeier, E. Improvement of soil fertility in historical ridge and furrow cultivation. *Geoarchaeology* **2022**, *37*, 750–767. [CrossRef]
29. Hänßler, E. *700 Jahre Albershausen*; Angebotene Zahlungsarten: Albershausen, Germany, 1975.
30. Ziegler, W. (Ed.) Vom frühen Mittelalter bis zur Neuzeit. In *Der Kreis Göppingen*; 1985; pp. 83–103.
31. Krähenmann, S.; Walter, A.; Brienen, S.; Imbery, F.; Matzarakis, A. Monthly, Daily and Hourly Grids of 12 Commonly Used Meteorological Variables for Germany Estimated by the Project TRY Advancement. Available online: https://doi.org/10.5676/DWD_CDC/TRY_BASIS_V001 (accessed on 5 January 2023).
32. Climate data. Station Göppingen. Daily Observations. 2021. Available online: https://opendata.dwd.de/climate_environment/CDC/observations_germany/climate/ (accessed on 5 January 2023).
33. Franz, M.; Arp, G.; Niebuhr, B. Schwarzjura-Gruppe. 2020. Available online: https://litholex.bgr.de/pages/Einheit.aspx?ID=10000049 (accessed on 5 January 2023).
34. Grams, G. Württembergische Landesvermessung in der Zeit von 1818-1840. In *200 Jahre Landesvermessung Baden-Württemberg*; Ministerium für Ländlichen Raum und Verbraucherschutz Baden-Württemberg, Ed.; 2018; pp. 19–32. Available online: https://www.lgl-bw.de/Ueber-Uns/Geschichte/200-Jahre-Landesvermessung/ (accessed on 5 January 2023).
35. IUSS Working Group WRB. *World Reference Base for Soil Resources: International Soil Classification System for Naming Soils and Creating Legends for Soil Maps*, 4th ed.; International Union of Soil Sciences (IUSS): Vienna, Austria, 2022.
36. Landesamt für Geoinformation und Landesentwicklung (LGL). Laserscandaten "ALS_2". Available online: https://www.lgl-bw.de/Produkte/3D-Produkte/Laserscandaten/ALS_2/ (accessed on 5 January 2023).
37. Fischer, F.; Winterrath, T.; Junghänel, T.; Walawender, E.; Auerswald, K. Mean Annual Precipitation Erosivity (R Factor) Based on RADKLIM Version 2017.002. 2019. Available online: https://doi.org/10.5676/DWD/RADKLIM_Rfct_V2017.002 (accessed on 5 January 2023).
38. Sauerborn, P. Die Erosivität der Niederschläge in Deutschland: Ein Beitrag zur Quantitativen Prognose der Bodenerosion Durch Wasser in Mitteleuropa. In *Bonner Bodenkundliche Abhandlungen*; Institut für Bodenkunde: Hanover, Germany, 1994; Volume 13.
39. Volker Hennings. *Erodierbarkeit der Böden in Deutschland*; Bundesanstalt für Geowissenschaften und Rohstoffe (BGR): Hannover, Germany, 2021.
40. Renard, K.G. *Predicting Soil Erosion by Water: A Guide to Conservation Planning with the Revised Universal Soil Loss Equation (RUSLE)*; United States Government Printing: Washington, DC, USA, 1997.
41. Efthimiou, N.; Psomiadis, E.; Papanikolaou, I.; Soulis, K.X.; Borrelli, P.; Panagos, P. A new high resolution object-oriented approach to define the spatiotemporal dynamics of the cover-management factor in soil erosion modelling. *CATENA* **2022**, *213*, 106149. [CrossRef]
42. Panagos, P.; Borrelli, P.; Meusburger, K.; Alewell, C.; Lugato, E.; Montanarella, L. Estimating the soil erosion cover-management factor at the European scale. *Land Use Policy* **2015**, *48*, 38–50. [CrossRef]
43. Auerswald, K.; Ebertseder, F.; Levin, K.; Yuan, Y.; Prasuhn, V.; Plambeck, N.O.; Menzel, A.; Kainz, M. Summable C factors for contemporary soil use. *Soil Tillage Res.* **2021**, *213*, 105155. [CrossRef]
44. Kokalj, Ž.; Hesse, R. *Airborne Laser Scanning Raster Data Visualization: A Guide to Good Practice*, 1st ed.; ZRC SAZU: Ljubljana, Slovenia, 2017; Volume 14.
45. Schmidt, J.; Werther, L.; Zielhofer, C. Shaping pre-modern digital terrain models: The former topography at Charlemagne's canal construction site. *PLoS ONE* **2018**, *13*, e0200167. [CrossRef]
46. Hesse, R. LiDAR-derived Local Relief Models—A new tool for archaeological prospection. *Archaeol. Prospect.* **2010**, *17*, 67–72. [CrossRef]
47. Hrabalikova, M.; Janecek, M. Comparison of different approaches to LS factor calculations based on a measured soil loss under simulated rainfall. *Soil Water Res.* **2017**, *12*, 69–77. [CrossRef]
48. van der Meulen, B.; Cohen, K.M.; Pierik, H.J.; Zinsmeister, J.J.; Middelkoop, H. LiDAR-derived high-resolution palaeo-DEM construction workflow and application to the early medieval Lower Rhine valley and upper delta. *Geomorphology* **2020**, *370*, 107370. [CrossRef]
49. Henselowsky, F.; Rölkens, J.; Kelterbaum, D.; Bubenzer, O. Anthropogenic relief changes in a long–lasting lignite mining area ("Ville", Germany) derived from historic maps and Digital Elevation Models. *Earth Surf. Process. Landf.* **2021**, *46*, 1725–1738. [CrossRef]

50. Deumlich, D. Beeinflusst Historische Landnutzung Die Aktuelle Bodenerosion? 2009. Available online: https://www.researchgate.net/publication/279416046_Beeinflusst_historische_Landnutzung_die_aktuelle_Bodenerosion (accessed on 5 January 2023).
51. Eyre, S.R. The curving Plough-strip and its Historical Implications. *Archaeol. Hist. Rev.* **1955**, *3*, 80–94.
52. Møller, P.G. Ridge and Furrow Fields: Field Systems ca. 1000–1800 as a Stabilising Factor in an Agricultural Society—A Danish Example. In *Agricultural and Pastoral Landscapes in Pre-Industrial Society*; Retamero, F., Schjellerup, I., Davies, A., Eds.; Earth Ser.; Oxbow Books: Philadelphia, PA, USA, 2015; pp. 159–171.
53. Panagos, P.; Borrelli, P.; Poesen, J.; Ballabio, C.; Lugato, E.; Meusburger, K.; Montanarella, L.; Alewell, C. The new assessment of soil loss by water erosion in Europe. *Environ. Sci. Policy* **2015**, *54*, 438–447. [CrossRef]
54. Panagos, P.; Borrelli, P.; Meusburger, K. A new European slope length and steepness factor (LS-Factor) for modeling soil erosion by water. *Geosciences* **2015**, *5*, 117–126. [CrossRef]
55. Panagos, P.; Ballabio, C.; Borrelli, P.; Meusburger, K.; Klik, A.; Rousseva, S.; Tadić, M.P.; Michaelides, S.; Hrabalíková, M.; Olsen, P.; et al. Rainfall erosivity in Europe. *Sci. Total Environ.* **2015**, *511*, 801–814. [CrossRef] [PubMed]
56. Niedertscheider, M.; Kuemmerle, T.; Müller, D.; Erb, K.H. Exploring the effects of drastic institutional and socio-economic changes on land system dynamics in Germany between 1883 and 2007. *Glob. Environ. Chang.* **2014**, *28*, 98–108. [CrossRef]
57. Grees, H. Zur Siedlungs- und Landschaftsentwicklung der Ostalb. Die Wüstungsvorgänge des ausgehenden Mittelalters und ihre Folgewirkung. *Karst Höhle* **1993**, 363–378.
58. Schreg, R. 15. Human Impact on Hydrology. In *The Power of Urban Water*; Chiarenza, N., Haug, A., Müller, U., Eds.; De Gruyter: Berlin, Germany, 2020; pp. 249–264. [CrossRef]
59. Landesanstalt für Landwirtschaft, Ernährung und Ländlichen Raum. Ertragsmesszahlen der Gemarkungen in Baden-Württemberg. Available online: https://www.lel-web.de/app/ds/lel/a3/Online_Kartendienst_extern/Karten/33279/index.html (accessed on 5 January 2023).
60. Scherer, S.; Deckers, K.; Dietel, J.; Fuchs, M.; Henkner, J.; Höpfer, B.; Junge, A.; Kandeler, E.; Lehndorff, E.; Leinweber, P.; et al. What's in a colluvial deposit? Perspectives from archaeopedology. *CATENA* **2021**, *198*, 105040. [CrossRef]
61. Scherer, S.; Höpfer, B.; Deckers, K.; Fischer, E.; Fuchs, M.; Kandeler, E.; Lechterbeck, J.; Lehndorff, E.; Lomax, J.; Marhan, S.; et al. Middle Bronze Age land use practices in the northwestern Alpine foreland—A multi-proxy study of colluvial deposits, archaeological features and peat bogs. *Soil* **2021**, *7*, 269–304. [CrossRef]
62. Diodato, N.; Borrelli, P.; Fiener, P.; Bellocchi, G.; Romano, N. Discovering historical rainfall erosivity with a parsimonious approach: A case study in Western Germany. *J. Hydrol.* **2017**, *544*, 1–9. [CrossRef]
63. Büntgen, U.; Franke, J.; Frank, D.; Wilson, R.; González-Rouco, F.; Esper, J. Assessing the spatial signature of European climate reconstructions. *Clim. Res.* **2010**, *41*, 125–130. [CrossRef]
64. Büntgen, U.; Brázdil, R.; Heussner, K.U.; Hofmann, J.; Kontic, R.; Kyncl, T.; Pfister, C.; Chromá, K.; Tegel, W. Combined dendro-documentary evidence of Central European hydroclimatic springtime extremes over the last millennium. *Quat. Sci. Rev.* **2011**, *30*, 3947–3959. [CrossRef]
65. Esper, J.; Büntgen, U.; Denzer, S.; Krusic, P.J.; Luterbacher, J.; Schäfer, R.; Schreg, R.; Werner, J. Environmental drivers of historical grain price variations in Europe. *Clim. Res.* **2017**, *72*, 39–52. [CrossRef]
66. Ließ, M.; Schmidt, J.; Glaser, B. Improving the Spatial Prediction of Soil Organic Carbon Stocks in a Complex Tropical Mountain Landscape by Methodological Specifications in Machine Learning Approaches. *PLoS ONE* **2016**, *11*, e0153673. [CrossRef] [PubMed]
67. Behrens, T.; Schmidt, K.; MacMillan, R.A.; Viscarra Rossel, R.A. Multi-scale digital soil mapping with deep learning. *Sci. Rep.* **2018**, *8*, 15244. [CrossRef]